sciendo

Studia Geotechnica et Mechanica, 2022; 44(3): 175–189

Original Study

Open Access

Salima Bouchemella*, Said Taibi

Effect of suction on the mechanical behaviour of unsaturated compacted clay–sand mixtures

https://doi.org/10.2478/sgem-2022-0016
received October 27, 2021; accepted March 21, 2022.

Abstract: In this work, a series of unconfined compression tests at different water contents were performed to investigate the mechanical behaviour of clay–sand mixtures compacted in standard Proctor conditions. For studying the effect of water content and suction on unconfined compressive strength (UCS) and on strain secant modulus (*E*50 modulus) of these mixtures, drying–wetting paths were defined by measuring the soil–water characteristic curves (SWCCs) using osmotic and salt solution techniques and filter paper method. The results highlighted that an increase in sand content of the mixture leads to an increase in the maximum dry densities and a decrease in the optimum water content of the materials. However, at the given state, when clay is mixed with 25% of sand, the UCS and *E*50 modulus increase to 37% and 70%, respectively, compared to those of clayey samples. But when clay is mixed with 50% of sand, the UCS and *E*50 modulus decrease to 38% and 46%, respectively, compared to those of clayey samples. The results also indicate that the UCS and *E*50 increase with a decrease in the water content and an increase in suction, irrespective of the sand content.

Keywords: Suction; Unsaturated soil; Clay–sand mixture; Unconfined compression strength; Strain secant modulus; Wetting–drying path.

1 Introduction

The sand–clay mixtures can be used for hydraulic barriers on slopes, as barriers for nuclear waste repositories or thermohydraulic backfills for geothermal boreholes. Moreover, the unsaturated compacted clay–sand mixtures can be used in civil engineering works such as construction of roads, dams and other types of embankments. They can be used also in raw earth building material. The sand–clay mixture is used generally in compacted fills and in compressed earth bricks (CEB) that require a high dry unit weight, as clay particles can fill the voids between sand particles. Further, mixing sand and clay (bentonite) may lead to a lower swelling pressure than that for clay alone [1]. Generally, the sand fraction is added to clayey soil to have a high shear strength or low compressibility or to reduce its swelling and the clay fraction is added to granular soil to reduce its permeability.

The behaviour of sand–clay mixture is governed by the granular phase when the sand matrix is predominant or by the cohesive phase when the clay matrix is predominant. Different studies were conducted to show the effect of sand or clay content on the behaviour of sand–clay mixtures. They generally showed that when sand was mixed with kaolin clay, the soil changed its behaviour from sand to clay. This clay content is enough to fill the voids of the granular portion at its maximum porosity. For example, Novais-Ferreira [2] described the existence of three zones of behaviour of the given sand–clay mixtures as a function of clay content: the first one, when the corresponding clay content is ≤28%, non-cohesive behaviour, where cohesion is negligible and the angle of friction is high (above 30°); the second one, when the clay content is between 28% and 41% (transition behaviour), where the soil is sensitive both to cohesion and the friction angle; the third one, when the clay content is ≥41%, cohesive behaviour, where cohesion is higher and the angle of friction is lower. However, Skempton [3] postulated for the clays that if the clay fraction is less than approximately 25%, the mixture behaves much like sand or silt rather than clay, but the residual strength is controlled almost entirely by the sliding friction of the clay minerals when the clay fraction is above 50%. Muir Wood and Kumar [4] demonstrated that the predominance of the mechanical behaviour of the clay matrix on the mechanical behaviour of the mixture occurs when the clay content is greater than 40% and the volume fraction of the granular constituent reaches about 0.45.

***Corresponding author: Salima Bouchemella,** INFRARES Laboratory, Department of Civil Engineering, University of Souk Ahras, E-mail: salima.bouchemella@univ-soukahras.dz
Said Taibi, LOMC, UMR CNRS 6394, Department of Civil Engineering, University of Le Havre Normandy

In recent years, many experimental tests and methods were conducted to study the hydro mechanical behaviour of sand–clay mixtures, such as the shear strength and the compression behaviour [4-13], the unconfined compressive strength (UCS) [14-18], the compaction characteristics [19-22] and the hydraulic properties [19, 23, 24]. In addition, the effect of suction and water content on the mechanical behaviour of sand–clay mixtures has also been investigated by many authors [13-17].

For shear strength, Vallejo and Mawby [5] showed that the shear strength is governed by the granular phase when the sand content is greater than 75% and by the cohesive phase when the sand content is lower than 40%. When the sand content is between 40% and 75%, the shear strength of the mixtures is partially controlled by the granular phase. Prakasha and Chandrasekaran [6] found that the inclusion of sand grains in a clay matrix leads to an increase in pore pressure resulting in a decrease in undrained shear strength, while Shafiee et al. [8] reported that the undrained shear strength increases with increasing sand content.

Likewise, Mun et al. [13] studied the impact of clay content on the undrained shear strength and on the compression curves of unsaturated sand–clay mixtures using the triaxial compression tests. The results indicated that sand–clay mixtures have lower undrained shear strength than sand or clay, but there is an intermediate rate of increase in shear strength with increasing strain rate, and the suction in the clay matrix has an important effect on the preconsolidation stress, which decreases as the percentage of clay increases. Pakbaz and Moqaddam [9] conducted consolidated-drained direct shear tests to study the effect of increasing clay content and the effect of gradation of sand on the behaviour of overconsolidated sand–clay mixtures and on their shear strength properties. The result of tests indicated that at a particular sand gradation, with an increase in clay content, the shear strength decreased. Also, at a constant clay content, the shear strength decreased with a decrease in sand grains' size. Cabalar and Mustapha [11] also studied the effect of particle gradation of sands with distinct shapes (rounded and angular) on the variation of the liquid limit (LL) and on the shear strength of clay mixed with different percentages of these sands. The results of the conducted tests indicated a decrease of undrained shear strength with an increase in the amount of sand. The use of rounded sands in a clay matrix leads to the development of higher undrained shear strength values, on which gradation of the sands has no effect.

In terms of UCS, Anuchit [15] studied the effect of sand content for different applied suctions and concluded that the UCS increased with increasing sand content for all the ranges of applied suction. For the effect of suction on UCS of clayey soils with different sand contents, the author found that the UCS increased with increasing matric suction for the matric suction range less than 50 kPa, but it decreased with increasing matric suction for the suction range greater than 50 kPa, whatever was the sand content in the mixture. Khan et al. [16] studied the compressive strength of compacted natural clay of high plasticity mixed with 20% and 40% of sand. The authors found that the compressive strength decreased with an increase in sand content because of increased material heterogeneity and loss of sand grains from the sides during shearing tests. The authors also showed that the compressive strength increased with decreasing water content of the material and for each sand–clay mixture, the compressive strength increased with an increase in density of the material. Sun et al. [14] carried out series of one-dimensional compression tests on the unsaturated compacted sand–bentonite mixture using suction-controlled oedometer. The results indicated that the yield stress increases and the compression index decreases with an increase of suction.

For compacted sand–clay mixture, some of the researchers investigated the effect of the percentages of sand and clay on the soil structure and the compaction properties (optimum water content and dry density values). For example, Kenney et al. [19] observed that there may be an optimal clay content that would lead to an increase in the dry density of a compacted sand–bentonite mixture. However, Howell et al. [20] concluded that the addition of clay may lead to an increase or decrease in the optimal water content and maximum dry density under the standard Proctor compaction effort according to the type of processed clay soil (water sorptivity and swelling potential), curing period and the mixing procedure. Cabalar and Mustafa [21] carried out California bearing ratio (CBR), unconfined compression strength (UCS) and compaction tests on various contents of sand and clay mixture. The results showed a decrease in UCS and an increase in CBR values with an increase in sand content.

The mixture with an appropriate sand content is generally used to valorise the fine raw earth to an eco-building material like compressed earth block (CEB) and to improve its hydromechanical behaviour defined by the UCS and the strain modulus. These parameters are measured generally when the CEB is made at a water content near saturation to reach the maximum density. However, the CEB dries before being implemented in the building. Therefore, the main objective of this paper is to study the behaviour of the compacted clay–sand mixtures

Table 1: Geotechnical properties of the tested soils.

Material	*Cc*	*Cu*	<80 µm, %	<2 µm, %	LL, %	PL, %	PI, %	*w*SPO, %	*ρd*max, g/cm³
Kaolinite 100K (Kheirbek-Saoud 1994) [33]	0.44	11.67	100	58	40	20	20	17.2	1.7
Sand	0.67	3,15	0	0	-	-	-	-	-
75K25S	0.25	25	77	43	31.7	18.5	13.2	15.8	1.77
50K50S	0.067	913.04	53	36	25.1	14.8	10.3	12	1.93

Cc: curvature coefficient, *Cu*: uniformity coefficient, LL: liquid limit, PL: plasticity limit, PI: plasticity index, *w*SPO: optimum water content in standard Proctor optimum SPO conditions, *ρd*max: maximum dry density

on the drying–-wetting paths, and then to investigate the influence of suction, water content and the added sand content on UCS and on the strain modulus of the compacted clay–sand mixture. To reach these purposes, series of unconfined compression tests at different water contents are performed on the kaolinite–sand mixtures compacted in standard Proctor properties. Furthermore, to link the water content to suction, the soil–water characteristic curves (SWCCs) of the compacted materials are highlighted by investigation of the effect of added sand percentage on the drying–wetting paths.

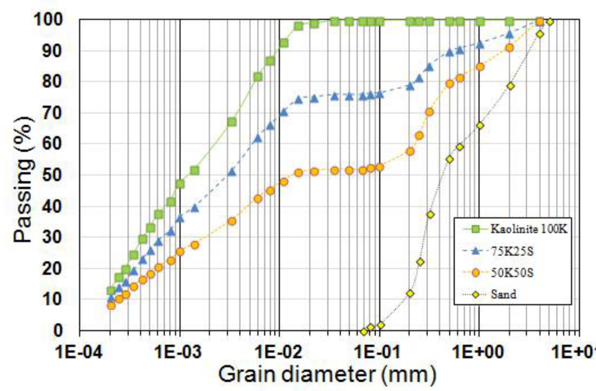

Figure 1: Grain size distribution curves of the tested soils.

2 Material characterisation

The clayey soils used in manufacturing of the building materials, dams and road embankments need to be amended generally with sand to meet the standards in strength and to reach the recommended behaviour. In this study, a commercial kaolinite (Sibelco, Hostun, France) noted 100K (100% kaolinite) is taken as a reference clayey soil. Two mixtures are prepared using this kaolinite and a French building commercial sand 0/4 provided by ULTIBAT and referenced ULTIBAT-91. These mixtures are noted as 75K25S (75% of kaolinite and 25% of sand) and 50K50S (50% of kaolinite and 50% of sand), respectively.

Many researchers have worked on the kaolinite 100K, both in terms of characterisation and mechanical behaviour [24-29]. Therefore, in this study, the lab experiments were focused on the soil properties of the mixture kaolinite–sand, such as the grain size distribution analysis, Atterberg limits and compaction. In accordance with the NF EN ISO 17892-4 [30] standard, the grain size distribution curves of the kaolinite 100K, sand and the mixtures 75K25S and 50K50S are shown in Fig. 1. The grain size disribution characteristic parameters are summarised in Table 1. The used sand is well-graded with a uniformity coefficient *Cu* of 3.15. The Atterberg limit

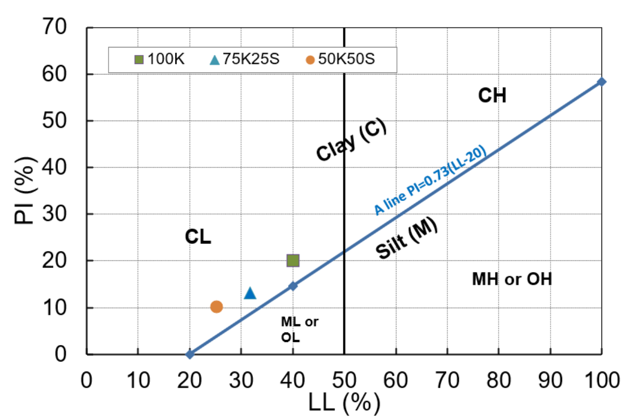

Figure 2: Atterberg limits of the tested soils.
LL: liquid limit, PI: plasticity index

tests were carried out in accordance with the NF EN ISO 17892-12 [31] standard to determine the liquid and plastic limits (LL, PL) of the soils. The results are plotted in Table 1. Fig. 2 presents the location of the kaolinite 100K and the mixtures 75K25S and 50K50S in Casagrande plasticity chart. These materials are classified as low plasticity clay. The LL and the plasticity index (PI) of the soil mixtures decrease with increasing sand percentage (SP) following

Table 2: Comparison between measured and correlated γdmax and wSPO.

Soils	LL,	Measured	Correlated	Error	Measured	Correlated	Error
	%	wSPO, %	wSPO, %	ΔwSPO, %	γdmax, kN/m³	γdmax, kN/m³	$\Delta\gamma d$max, kN/m³
100K	40	17.2	18.5	1.3	17	16.9	0.1
75K25S	31.7	15.8	15.4	0.4	17.7	17.7	0
50K50S	25.1	12	12.8	0.8	19.3	18.3	1.0

LL: liquid limit

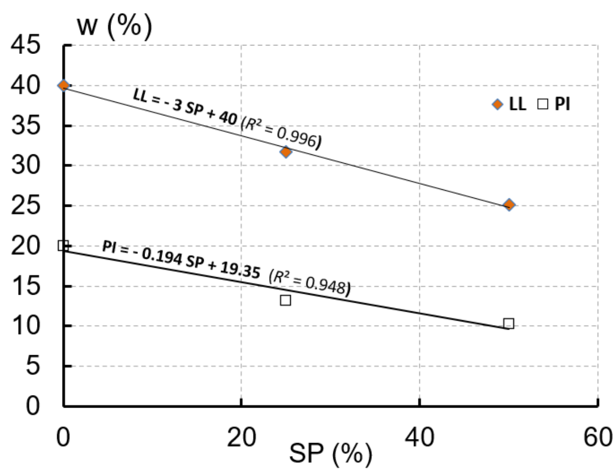

Figure 3: LL and PI versus SP.
LL: liquid limit, PI: plasticity index, SP: sand percentage

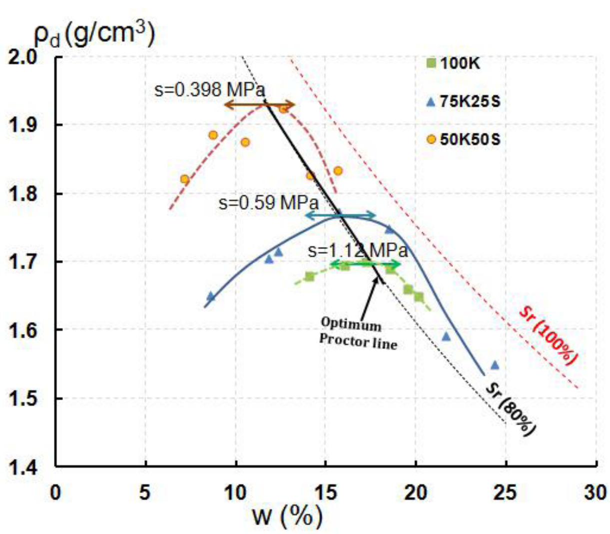

Figure 4: Compaction characteristics for the kaolinite 100K and 75K25S, 50K50S mixtures.

a linear function as illustrated in Fig. 3. A similar linear variation was also reported previously [7, 11, 32]. Monkul and Ozden [7] found the same slope of the line PI (SP) which is equal to about 0.19 (%/%).

Standard Proctor tests were conducted in accordance with Afnor NF P 94 093 [34] standard. The curves highlighted the relationship between water content and dry density curves of the kaolinite 100K, and the mixtures are presented in Fig. 4. The Proctor optimum water contents and the maximum dry densities (wSPO, ρdmax) of the soils were determined. The optimum Proctor line and the saturation curves are also plotted in Fig. 4.

The optimum water contents and maximum dry densities of the soils are presented in Table 1. The kaolinite 100K showed a maximum dry density of 1.7 g/cm³ at an optimum water content wSPO equal to 17.2%, which is close to PL = 20%. These data are similar to those reported by Khan et al. [16], Azam and Chowdhury [35] and Marinho and Oliveira [36]. Marinho and Oliveira [36] reported that for cohesive soils, the optimum water content is within ±5% of the PL. It can be observed from Fig. 4 that an increase in sand content decreases the void ratio of the mixture, and thus increases its dry density from 1.7 g/cm³ (case 100K) to 1.77 and 1.93 g/cm³ for 75K25S and 50K50S, respectively. The same trend was observed by Khan et al. [16].

Fig. 4 shows that this increase in density due to the increase of sand content needs lower water content (wSPO). It also shows that, the optimum Proctor line and the 80% saturation curve are superposed, which reveals that the three soils are quasi-saturated at this state. Based on the analysis of dozens of soils around the world, Fleureau et al. [26] proposed correlations of some parameters of fine soils compacted at the optimum Proctor. These correlations link the optimal dry unit weights (γdmax) and the water contents to the LL as presented by Eqs 1 and 2.

$$w_{SPO} = 1.99 + 0.46\,LL - 0.0012\,LL^2 \qquad (1)$$

$$\gamma_{dmax} = 21 - 0.113\,LL + 0.00024\,LL^2 \qquad (2)$$

Therefore, in this section, the measured maximum dry unit weights and the optimum water contents in SPO of the studied soils were compared to the correlated values as shown in Table 2, to verify the obtained values. A good agreement was observed between the measured and the correlated values.

3 Methods

To determine the hydromechanical properties of sand–kaolinite mixtures, two different types of tests were conducted. The first one concerned the UCS test carried out on samples prepared in standard Proctor conditions (*ρd*max and *w*SPO). The second one concerned the study of drying–wetting paths and of SWCC using different techniques.

3.1 The UCS test

The UCS tests were carried out according to the standard NF EN ISO 17892-7 [37]. The Kaolinite 100K and the mixtures 75K25S and 50K50S were first air dried and then wetted to the standard optimum water content *w*SPO and kept in a sealed bag for 24 h to homogenise the water content. Afterwards, the soils were compacted under quasi-static loading to reach *ρd*max in a specific mould using top and bottom pistons simultaneously. This technique produces uniform and homogeneous samples and limits the density gradient along the z axis of the samples (Fig. 5). The specimens were cylindrical with a diameter of 50 mm and a height of 100 mm (Fig. 5), so a slenderness ratio equal to 2 was obtained, which was within the range (2.0–2.5) specified by the standard NF EN ISO 17892-7 [37]. After compaction, the specimens were wrapped in a waterproof plastic film and stored for 24 h. This allows the water content to homogenise within the compacted sample. Then, the UCS tests were carried out at a slow constant displacement rate of 0.0203 mm/min until failure, using an electromechanical press to avoid any dynamic effect. Finally, the water content was measured after failing.

From the stress–strain curve (*q*(*ε1*)) of kaolinite and mixture samples, a strain modulus noted '*E*50', presented in Fig. 6, is then defined according to the standard NF EN ISO 17892-9 [38] as follows:

- The point corresponding to 50% of the maximum strength of the material is located on the stress–strain curve.
- Then the secant line through the origin of the axes and through this point is drawn.
- The slope of this secant line represents the large strain secant modulus called *E*50 modulus [39].

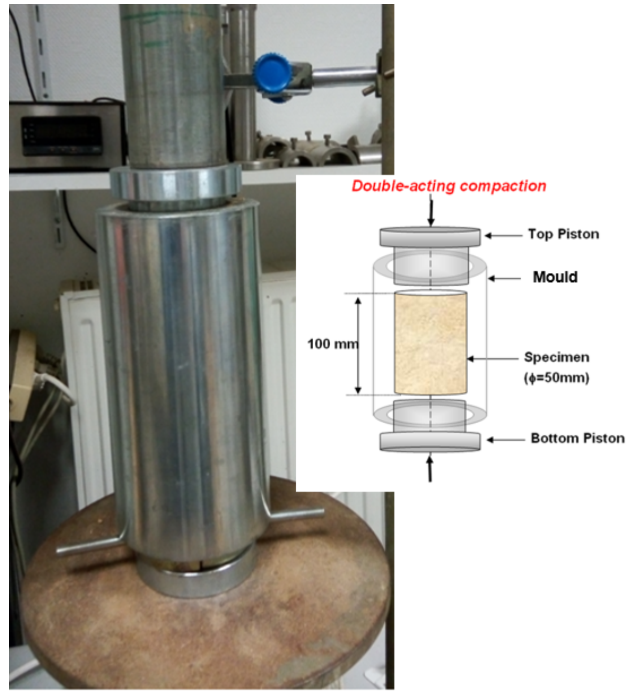

Figure 5: Compacted sample device.

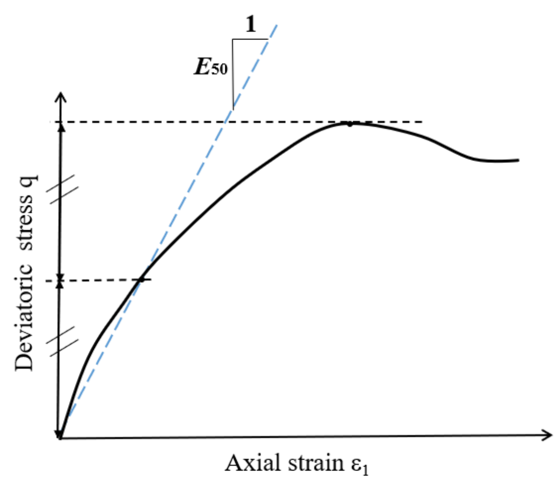

Figure 6: *E*50 modulus definition.

3.2 Drying–wetting paths

SWCC is a representation of the fundamental behaviour of soil matric suction with moisture content property. SWCC is generally completed with the variation of void ratio corresponding to the water content and suction curves. In the present research, to measure the water retention behaviour of the soil in a wide range of suction, different controlled and measured suction techniques are used to determine the drying–wetting paths of samples compacted at the standard optimum state. These methods are summarised as follows:

– tensiometric plates to impose suctions from 1 to 20 kPa [40, 41],
– osmotic method for suctions ranging from 50 to 1500 kPa [17, 22, 42-45],
– salt solutions for higher suctions ranging from 600 kPa to 400 MPa [17, 40, 41, 46, 47] and
– filter paper method is used to measure the suction corresponding to the standard optimum water content [17, 47, 48].

3.2.1 Controlled suction techniques

Tensiometric plates are made of a low-porosity sintered glass (or ceramic) filter set in a glass funnel and saturated with de-aired water. The plates play the role of a semi-permeable separation. They are in contact with a reservoir and a measurement column also filled with de-aired water. The specimens are placed on the filter and a negative pore water pressure (or suction) with respect to the atmospheric pressure is imposed in the column by the difference in height between the specimen and the free end of the column.

In the osmotic method, the specimen is placed in contact with a solution of large-sized molecules of polyethylene glycol (PEG 6000) through a semi-permeable membrane with pores smaller than 5 nm. The membrane allows only the passage of water. Due to a difference in the concentration of the solution across the membrane, water flows from lower concentrations to higher ones. This results in the application of matrix suction to the soil, which increases with the concentration of PEG. When equilibrium is reached, the hydration potential of PEG is equal to that of the soil. The relationship between the applied suction and PEG concentrations is deduced from a parabolic relation proposed by Delage et al. [46] as follows:

$$s = 11\,C^2 \tag{3}$$

where s is the suction expressed in MPa and C is the concentration of PEG expressed as grams of PEG per gram of water.

The salt solutions technique consists in enclosing the samples in desiccators containing different salt solutions (KNCS, K2SO4, NaNO2, NaCl, CuSO4) to control the relative humidity of the atmosphere, and therefore the suction in the specimens. This allows humidity exchanges between the atmosphere and soil until equilibrium. Total suction applied is related to the imposed relative humidity by Kelvin law (Eq. 4) as follows:

$$s = \frac{\rho_w . R . T}{M_v} \ln(RH) \tag{4}$$

where s: the total suction (MPa), ρw: the density of water at temperature T (g/cm³), R: perfect gas constant (R = 8.314 J/mol K), T: temperature (K), Mv: molecular weight of water vapour (Mv = 18.01 g/mol) and RH: relative humidity (%).

3.2.2 Measured suction technique

The initial suction of compacted samples corresponding to the optimum water content is measured using the filter paper method according to the standard ASTM D5298-16 [48]. The value of matric suction is derived from the water content of calibrated filter paper referenced Whatman N°42, which is protected on both sides by two ordinary filter papers and placed in contact with the soil specimens during compaction test. Afterwards, the filter paper is enclosed with soil specimen in an airtight container until moisture equilibrium is established. The filter paper (Whatman N°42) is then extracted and its water content is measured immediately to avoid evaporation.

For all the used techniques, once the moisture equilibrium state is reached, the water content and the total volume of the specimen are measured by immersion in a non-wetting oil (commercial Kerdane), followed by drying in an oven at 105°C for 24 h, allowing the void ratio (e) and degree of saturation (Sr) of the material to be calculated. The obtained parameters (w, e, Sr) are related to the imposed and measured suctions.

3.2.3 Specimen preparation

The drying–wetting path tests were carried out on samples compacted at the standard optimum water content to the corresponding maximum dry density. The preparation technique of the compacted samples is explained in section 3.1. Each sample was cat into small cubes of about 2cm³ to be tested.

4 Results and Discussion

4.1 Drying–wetting paths

The hydromechanical behaviour of the material can be studied by the drying–wetting path tests. Fig. 7 summarises all the results of drying–wetting tests performed on samples compacted in SPO. These results are represented in five corresponding diagrams: a) void ratio versus water content; b) void ratio versus suction; c) degree of saturation versus water content; d) degree of saturation versus suction and e) water content versus suction. The values of the initial suction (*si*) of samples compacted in SPO measured by the filter paper method are compared, as shown in Table 3, to the values of suction deduced from Fleureau et al. [26] correlations according to the LL, as shown in Eq. (5). This comparison reveals a good agreement between these correlations and the measured values.

$$s_{SPO} = 1.72\ (\mathrm{LL})^{1.64} \tag{5}$$

Fig. 7a and b presents the volume change behaviour of the soil under the effect of the water content and suction, respectively. As shown in Fig. 7b, the results indicate that the value of the initial measured suction of samples (*si*) of each material, which is equal to 1.12, 0.59 and 0.398 MPa for 100K, 75K25S and 50K50S, respectively, is close to the suction value corresponding to its shrinkage limit (*ssl*) (1.3, 1.0 and 0.63 MPa for 100K, 75K25S and 50K50S, respectively). The initial void ratio values (*ei*), which are equal to 0.67, 0.59 and 0.4 for 100K, 75K25S and 50K50S, respectively, are also close to the void ratio values of shrinkage limit (*esl*) (0.64, 0.55 and 0.38 for 100K, 75K25S and 50K50S, respectively), which means that the shrinkage effect in the compacted samples is not significant. However, the value (*esl*) of kaolinite decreases from 14% to 40% when the SP increases from 25% to 50% in the mixture. It must be noted that when the applied suction is higher than the initial one, the samples follow a drying path and when it is lower, they follow a wetting path.

The relationships between the void ratio (*esl*), water content (*wsl*) and suction (*ssl*) of shrinkage limit versus SP can be represented fairly by a linear relation as presented in Fig. 8a, b and c, respectively. It is observed that when the imposed suction (*s*) is higher than *si*, drying of the three compacted samples follows the level of shrinkage limit. However, for the wetting paths obtained by imposing suctions lower than *si*, the three materials follow the overconsolidated (OC) line. On comparing the path of slurry and compacted samples of the kaolinite 100K represented in Fig. 7b, it can be observed that for a suction (*s*) range less than that of the initial one (*si*), the compacted samples follow the OC line, while for a suction range higher than *si*, the samples follow the shrinkage plateau because the initial suction is closer to the shrinkage limit. For a slurry in which *wi* is equal to 1.5 LL, the application of increasing suctions causes a decrease in the void ratio, which changes significantly following the normally consolidated (NC) line.

On the wetting path, when the water content is greater than the optimum water content values (*w*SPO), the variation of the void ratio corresponding to the water content is almost linear for the three materials, as shown in Fig. 7a. Under these values, the decrease in the void ratio is very small until it becomes constant (equal to *esl*), while the water content continues to decrease.

From the *Sr(w)* and *Sr(s)* curves shown in Fig. 7c and d, respectively, it is observed that during the wetting process, the three soils reached approximately close degrees of saturation, which did not exceed 93%, regardless of the sand content. On the other side, Fig. 7e shows that the kaolinite 100K has a higher saturation water content (*ws* = 29.6%) than those of the mixtures (*ws* = 23.8% for 75K25S and *ws* = 16.7% for 50K50S). This difference in saturated water content is explained by the differences in void ratio of each soil at the saturation state, which are 0.88, 0.72 and 0.57 for 100K, 75K25S and 50K50S, respectively (Fig. 7a, b). The decrease in void ratio is due to an increase in sand content, as reported by [7].

The same general behaviours of the changes in void ratio, water content and degree of saturation versus suction or water content of the studied soils were observed by Serbah et al. [17] and Fleureau et al. [26] when they carried out an investigation to relate the drying–wetting paths of soils and their LLs.

Table 3: Initial conditions of drying–wetting test.

Material	LL,	*w*SPO,	*ρd*max,	*si* measured,	*si* correlated,
	%	%	g/cm³	MPa	MPa
100K	40	17.2	1.7	1.12	0.729
75K25S	31.7	15.8	1.77	0.59	0.644
50K50S	25.1	12	1.93	0.398	0.339

LL: liquid limit

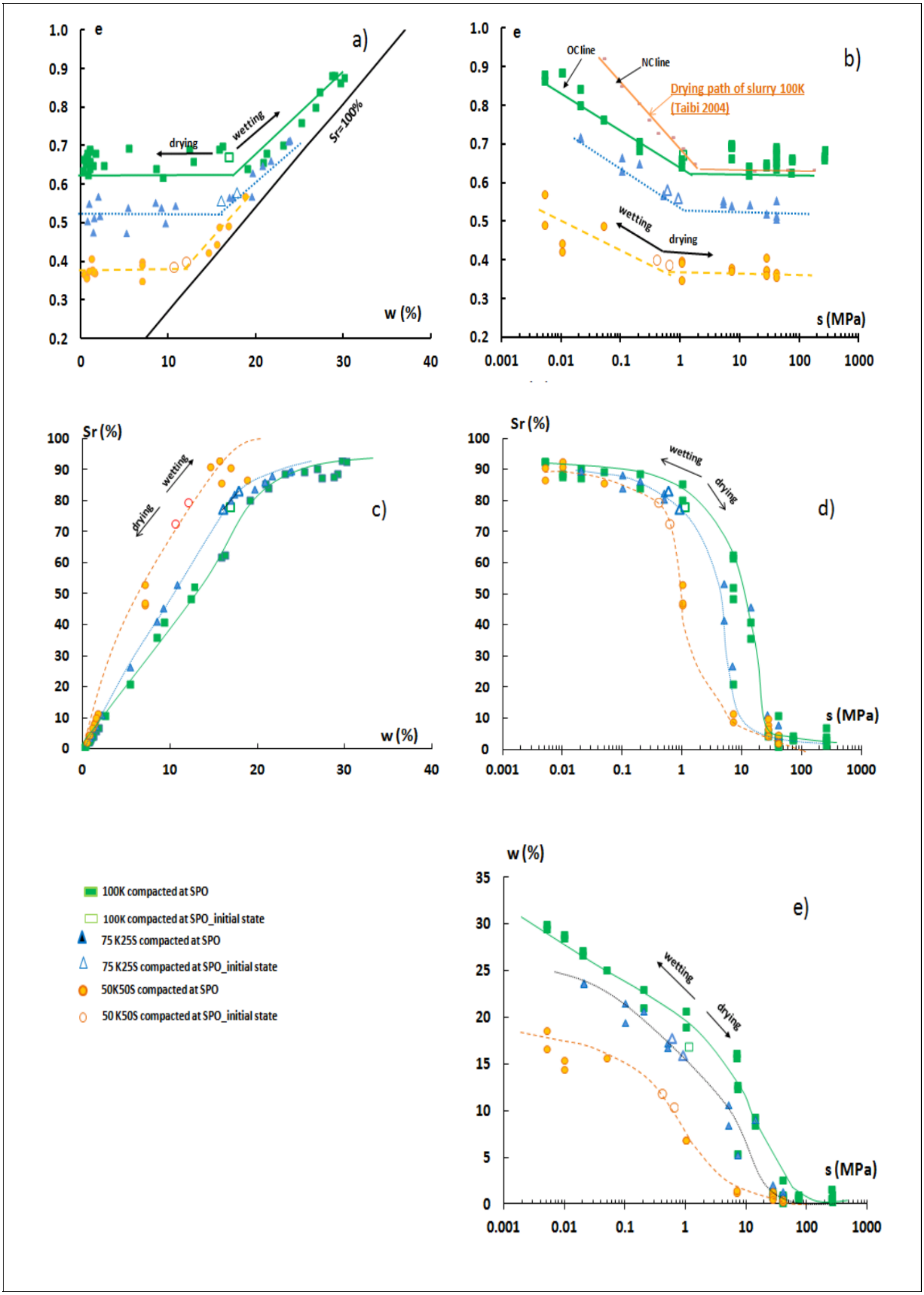

Figure 7: Wetting–drying paths of compacted samples of kaolinite 100K and mixtures 75K25S and 50K50S.

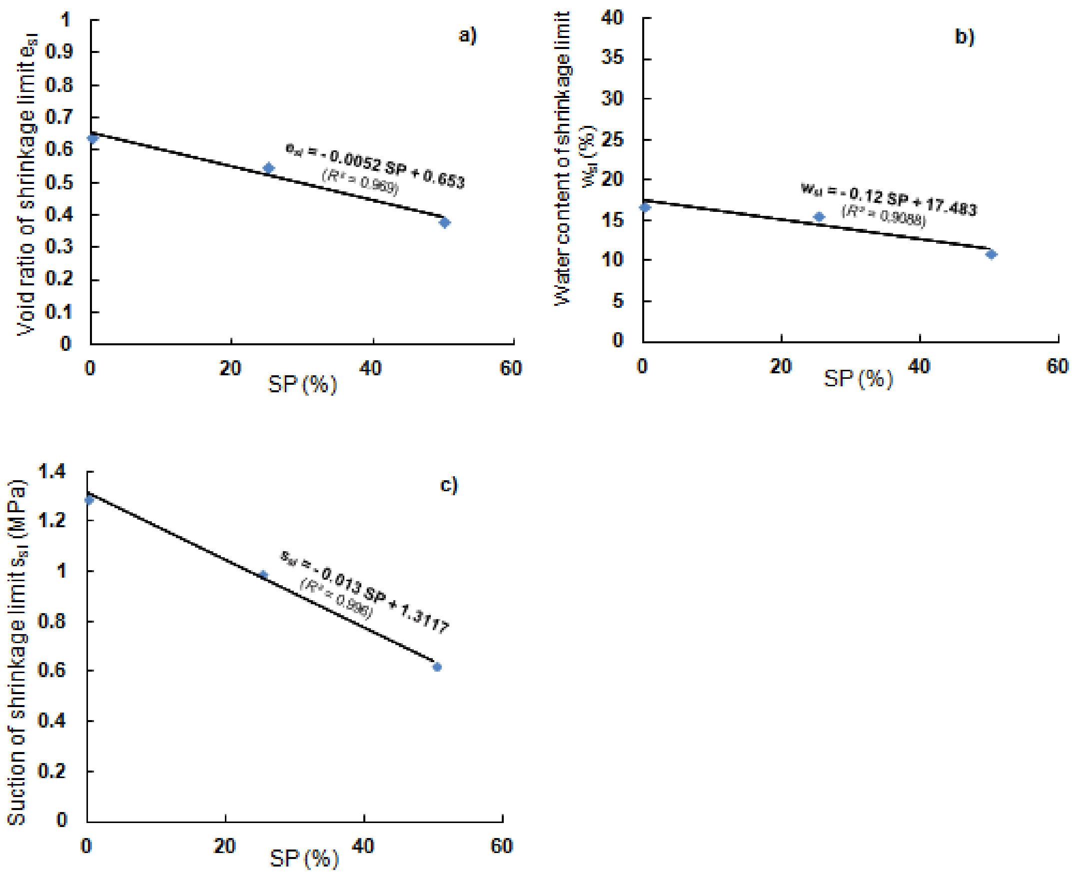

Figure 8: The relationship between: a) void ratio e_{sl}, b) water content *w*sl and c) suction *ssl* of shrinkage limit versus SP.
SP: sand percentage

From the wetting path of 14 clayey soils compacted under the standard Proctor optimum conditions, Fleureau et al. [26] showed a good linearity in the plane [log (s), e] and [log(s), w] and defined the slopes of the planes (*Cms*) and (*Dms*), respectively, from LL as follows:

$$C_{ms} = \frac{-\Delta e}{\Delta(\ln(s))} = 0.029 - 0.0018LL + 5\ 10^{-6}LL^2 \quad (6)$$

$$D_{ms} = \frac{-\Delta w}{\Delta(\ln(s))} = 0.54 - 0.030LL + 3.3\ 10^{-6}LL^2 \quad (7)$$

Figs 9 and 10 show the relationship between suction and the void ratio and the normalised water content respectively for wetting path of the studied soils and a set of 14 clayey soils compacted at *w*SPO. For suction between 0.1 and 1000 kPa, the wetting path of studied soils (100K, 75K25S and 50K50S) showed good linearity in the plane [log (s), e] and were well located in correlated lines according to LL (Fig. 9).

In the plane of suction versus normalised water content [log (s), w/Dms] (Fig. 10), the wetting paths of studied mixtures were located inside the single spindle of points, as suggested by the study of Fleureau et al. [26].

4.2 Effect of added sand on large strain behaviour of compacted samples

4.2.1 On UCS

The relationship between the deviatoric stress q and the axial strain ε1 at standard water content *w*SPO and maximum dry density *ρd*max is plotted in Fig. 11a. Fig. 11b presents the variation of the average values of UCS corresponding to the SP. The results show that the maximum UCS of the kaolinite 100K is equal to 0.47 MPa. It is observed that when the kaolinite 100K is mixed with 25% of sand, its UCS increases to 0.6 MPa, which represents an increase of about 37%. But when it is mixed with 50% of sand, the UCS decreases to 0.29 MPa, which represents a

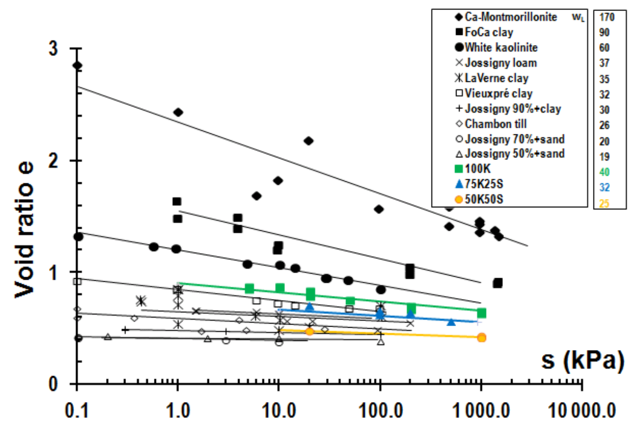

Figure 9: Void ratio for wetting paths of different soils compacted in SPO conditions.

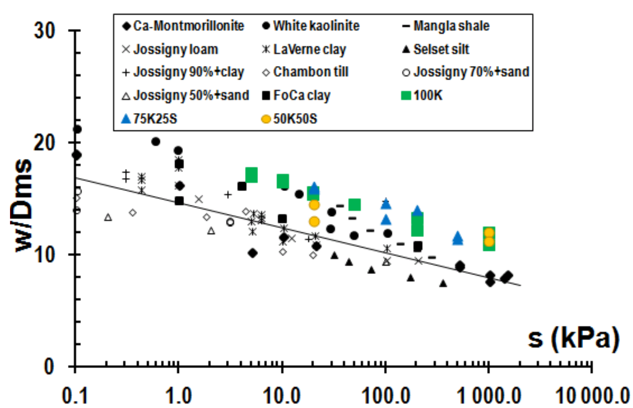

Figure 10: Normalised water contents for the wetting paths of different soils compacted in SPO conditions.

decrease of 38% compared to the compressive strength of 100K. The test results reveal that there is an optimum SP where the UCS is maximum; any further increase in sand content is not, in any way, beneficial to strength gain. Typical behaviour was observed by Muhwezi and Achanit [49] for stabilised CEB blended with sand; the optimum SP in their study was about 10%. However, this trend was not consistent as Khan et al. [16] found that the compressive strength decreased with an increase in sand content for natural clay of high plasticity mixed with 20% and 40% sand. But Anuchit [15] obtained contrasting results, which revealed that for kaolin clay mixed with 0, 20% and 40% silica sand, the UCS increased with increasing sand content.

The increase and then a decrease in UCS with an increase in the added sand content, as observed in Fig. 11b, can be explained as follows.

– The behaviour of the pure kaolinite 100K is essentially governed by the effective cohesion (the apparent cohesion) of the material noted 'C', which is given by Mohr–Coulomb criterion, and it is important for this high plastic material. The strength of the material is, therefore, mainly due to cohesion and not friction between the clay particles.
– When this kaolinite is mixed with 25% of sand, this added sandy granular fraction generates a granular friction between the particles, and with the remaining high percentage of kaolinite (75%), cohesion does not decrease significantly with the addition of 25% of sand. Consequently, the behaviour of the mixture is that of a sandy clayey soil. Therefore, the strength is due to both the effective cohesion of the kaolinite and the friction generated by the added sand fraction. Hence, an increase in UCS is observed.
– When the percentage of the added sand becomes important (50%), cohesion of the mixture decreases significantly and the observed behaviour is that of a clayey sand, in other words, dominated by the sand fraction, whose strength is essentially due to the capillary cohesion generated by the water meniscus between the grains. Because the UCS due to capillary cohesion is much lower than the UCS due to effective cohesion of the kaolinite, this may explain the drop in strength observed for the mixture 50K50S.

Furthermore, Mullins and Panayiotopoulos [50] and Khan et al. [16] showed that the decrease in compressive strength in mixture samples with high sand content can be explained by the increase in material heterogeneity, and the failure plane had to pass through the weakest zone in the sample [50].

4.2.2 On *E*50 modulus

The *E*50 modulus of clayey and mixture samples compacted under the standard Proctor conditions is deduced from the USC *(ε1)* curve, as discussed in section 3.1. The variation of the average values of *E*50 modulus versus SP is presented in Fig. 12. The figure shows first the increase in *E*50 modulus from 42 to 71.5 MPa when 25% of sand is added, and then the *E*50 modulus decreases to 22.5 MPa when 50% of sand is added. This evolution is the same as for USC results.

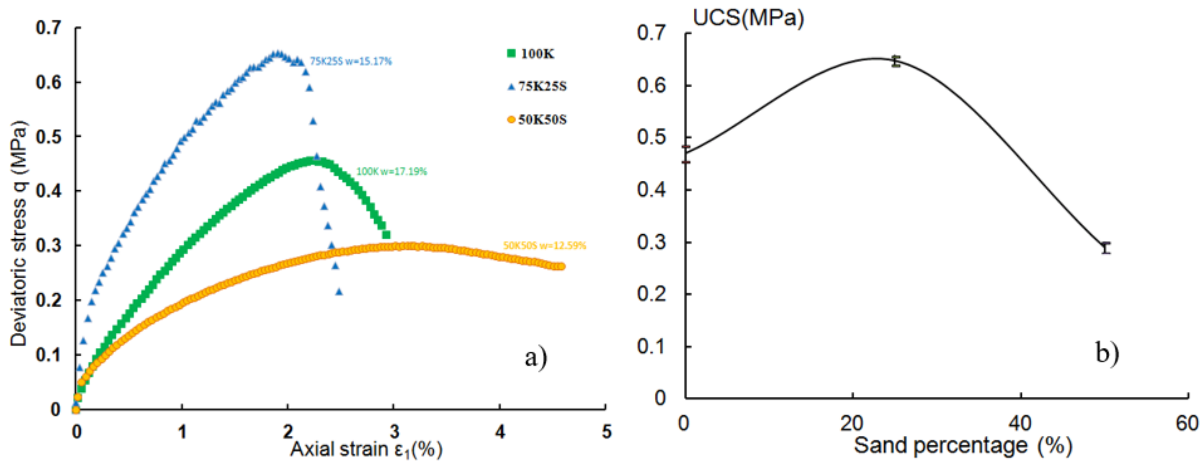

Figure 11: Relationship between a) deviatoric stress and axial strain for kaolinite and mixture samples, b) UCS and sand percentage, in SPO conditions. UCS: unconfined compressive strength.

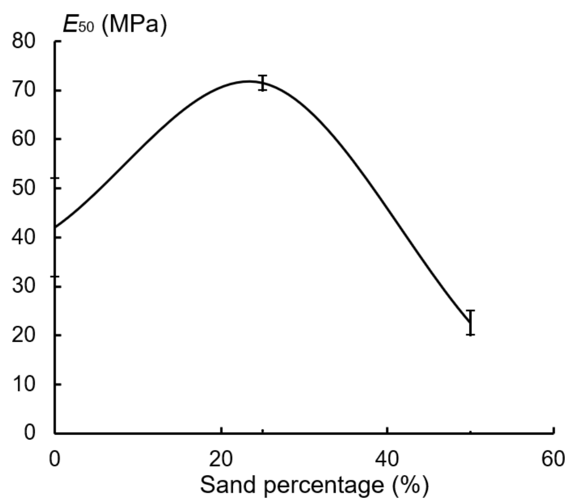

Figure 12: Relationship between *E*50 modulus and sand percentage for kaolinite and mixture samples in SPO conditions.

4.3 Effect of water content and suction on UCS and *E*50 modulus

To study the effect of the water content and suction on UCS and *E*50 modulus of the compacted samples, series of UCS tests were conducted on the samples, which were initially performed in standard water content (*w*SPO) for each soil. Then the soil samples were air-dried to the required value of water content corresponding to a given matric suction.

Cylindrical samples were placed under a bell jar in a horizontal position to allow slow evaporation and avoid gravity flow. The average time varied from 1 to 3 weeks, depending on the target water content. Once the target water content was reached, the samples were wrapped in cellophane film and placed in an airtight bag for 48 h in a horizontal position to homogenise the water content within the specimen. After these steps, the samples were subjected to mechanical loading (UCS test).

It should be noted that during this drying phase, no significant shrinkage of the specimens was observed. In fact, the initial state of compaction 'standard Proctor optimum' was very close to the shrinkage limit, as shown in Fig. 7a and b.

Fig. 13a and b shows the variation of UCS versus water content and suction, respectively, for kaolinite 100K and the mixtures 75K25S and 50K50S. It can be observed that the UCS increased with decreasing water content and increasing suction, irrespective of the added sand content. It can be also deduced that the UCS increases when the kaolinite is mixed with 25% of sand and decreases when it mixed with 50% of sand, irrespective of the water content or suction of the samples. The 50K50S curve is located between 100K and 75K25S curves, according to Fig. 13a and b.

In fact, a decrease in water content increases the suction, thus increasing the capillary cohesion, which induces an increase in material strength.

The variations of *E*50 modulus of the clay 100K and the mixtures versus water content and suction are shown in Fig. 14a and b, respectively. Regardless of the sand content, it can be observed that the *E*50 modulus decreases when the water content increases, and it increases when the suction increases; similar behaviour was observed by Serbah et al. [17]. Different from what is observed at an optimum state, the *E*50 modulus of the 50K50S samples becomes larger than the *E*50 modulus of the 100K samples when the suction is greater than 1 MPa.

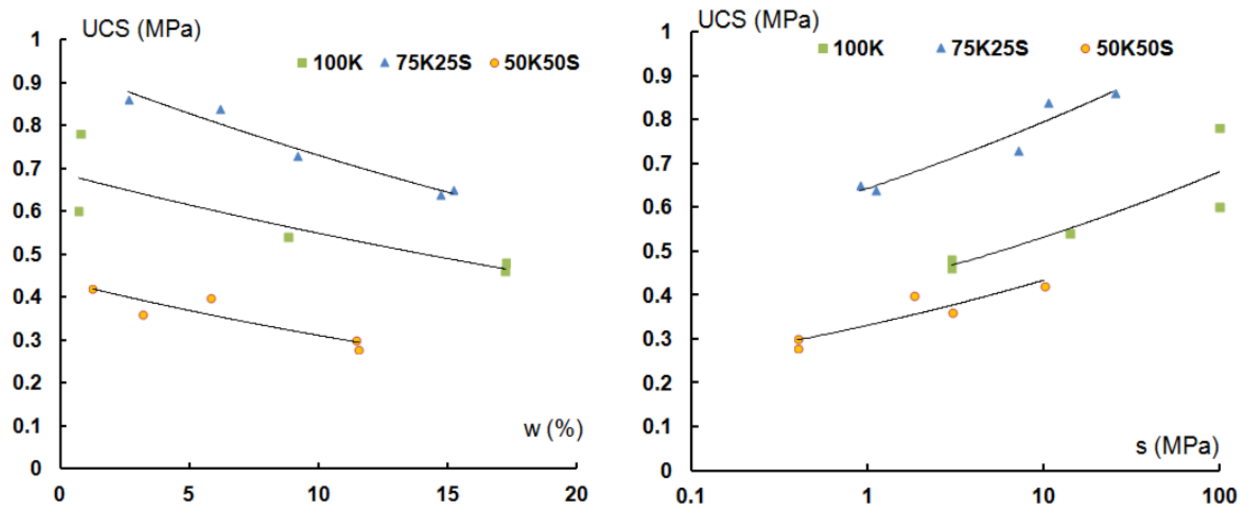

a) UCS versus water content

(b) USC versus suction

Figure 13: Relationship between UCS and a) water content, b) suction for 100K and mixture samples.. UCS: unconfined compressive strength

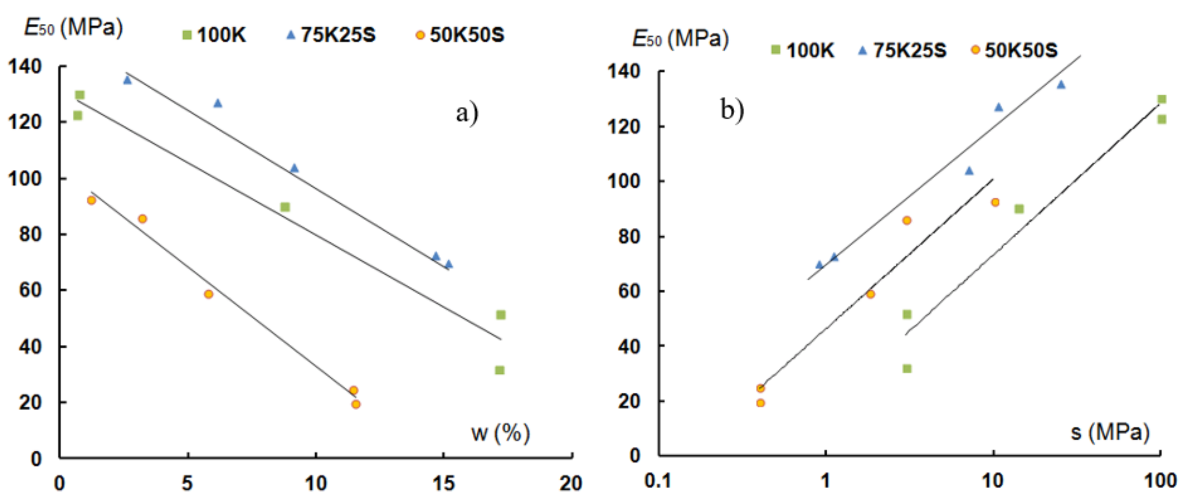

a) *E*50 versus water content

(b) *E*50 versus suction

Figure 14: Relationship between *E*50 modulus and a) water content and b) suction for 100K and mixture samples.

The change in the location of the curves of 100K and 50K50S when interpreted with suction concludes that when the water content varies, the main parameter to describe the mechanical behaviour of unsaturated soil is suction or the negative pressure and not the water content, which is a physical parameter. It is also true for UCS curves; when UCS is interpreted with suction (Fig. 14b), the gap between the curves of 100K and 50K50S observed with the water content in Fig. 14a is significantly reduced, from 0.3 MPa for a given water content to 0.1 MPa for a given suction.

Fig. 15 presents the variation of *E*50 modulus with UCS for all the mixtures. It is observed that whatever was the percentage of the added sand, the *E*50 modulus increased with an increase in UCS following a linear law expressed by *E*50 = 156.73 UCS.

5 Conclusions

In this study, the effect of suction and granular fraction content on the mechanical properties of the unsaturated fine material was studied. The unconfined axial compressive loading tests were performed on different clay–sand mixtures prepared under standard Proctor conditions (ρdmax and *w*SPO), and then, the soil samples

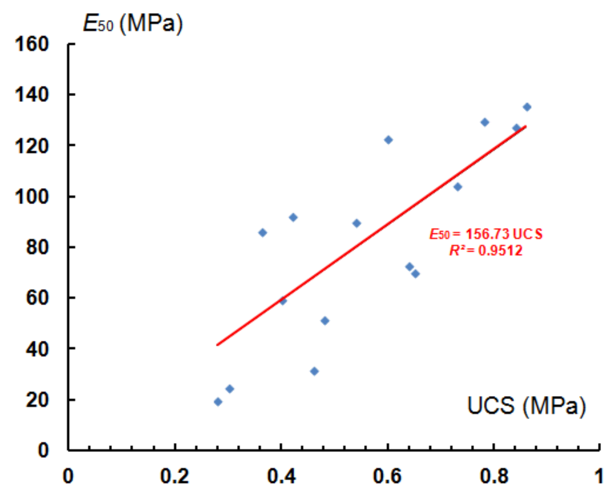

Figure 15: Relationship between *E*50 modulus and UCS. UCS: unconfined compressive strength.

were air-dried to the required value of water content to characterise the evolution of the UCS and the strain secant modulus with the percentage of the added sand and the water content. In addition, the relationship between the water content and suction (SWCC) has been highlighted through the development of drying–wetting curves, which allows the effects of suction on UCS and on strain secant modulus to be described.

The compaction tests reveal that an increase in sand content contributes to a decrease in the void ratio, and hence to an increase in the density of the mixture and decrease in the corresponding optimum water content. The drying–wetting curves show that the shrinkage limit decreases with the increase in percentage of the added sand, and consequently increases with the LL of mixtures.

The main results of the added SP effect at a given state (water content, density and suction) highlight the following:

– When clay is mixed with 25% of sand, the UCS and *E*50 modulus of 75K25S samples increase to 37% and 70%, respectively, compared to those of clayey samples. The increase in strength is due to both the effective cohesion of the kaolinite and the friction generated by the added sand fraction.
– When clay is mixed with 50% of sand, the UCS and *E*50 modulus of the 50K50S samples decrease to 38% and 46%, respectively, compared to those of clayey samples. This can be explained by the fact that, as the material is unsaturated, the strength due to the capillary cohesion of sand fraction is much lower than the strength due to the effective cohesion of the kaolinite fraction, which may explain the drop in UCS observed for the mixture 50K50S.

In the case of the unsaturated soils, the evolution of the mechanical parameters (UCS, *E*50) is governed by suction, which is a mechanical parameter, and not by the water content, which is a physical parameter. The suction decreases the void ratio and increases both the UCS and the *E*50 modulus. A unique linear relationship linking the *E*50 modulus to the UCS is highlighted, irrespective of the sand content.

References

[1] [1] Komine, H. and Ogata, N. (1999). Experimental study on swelling characteristics of sand-bentonite mixture for nuclear waste disposal, Soils and found. 39(2), pp. 83-97. DOI:10.3208/sandf.39.2_83
[2] Novais-Ferreira, H. (1971). The clay content and the shear strength in sand-clay mixtures. Proceeding of 5th African Regional Conference of Soil Mechanic. Found. Eng. Luanda, August.
[3] Skempton, A.W. (1985). Residual strength of clays in landslides, folded strata and the laboratory, Géotechnique, 35(1), pp. 3-18; DOI: 10.1680/geot.1985.35.1.3
[4] Muir Wood, D. and Kumar, G. V. (2000). Experimental observations of behaviour of heterogeneous soils, Mec. Cohesive-Frictional Mater., 5(5), pp.373–398. DOI:10.1002/1099-1484(200007)5:5
[5] Vallejo, L. E. and Mawby, R. (2000). Porosity influence on the shear strength of granular material-clay mixtures, Eng. Geol., 58(2), pp. 125–136. DOI:10.1016/S0013-7952(00)00051-X.
[6] Prakasha, K. S. and Chandrasekaran, V. S. (2005). Behaviour of marine sand-clay mixtures under static and cyclic triaxial shear, J. Geotech. Geoenviron. 131(2), pp. 213–222. DOI:10.1061/(ASCE)1090-0241(2005)131:2(213)
[7] Monkul, M.M. and Ozden, G. (2007). Compressional behavior of clayey sand and transition 20 fines content, Eng. Geol., 89(3–4), pp. 195-205, https://doi.org/10.1016/j.enggeo2006.10.001.
[8] Shafiee, J., Tavakoli, H.R. and Jafari, M.K. (2008). Undrained behaviour of compacted sand-clay mixtures under monotonic loading paths, J. Appl. Sci., 8(18), pp. 3108–3118.
[9] Pakbaz, M. S. and Moqaddam A.S. (2012). Effect of sand gradation on the behaviour of sand-slay mixtures, Int. J. GEOMATE. 3(1) (Sl. No. 5), pp. 325-331. DOI: 10.21660/2012.5.3d.
[10] Cabalar, A.F., Hasan, R.A. (2013). Compressional behaviour of various size/shape sand–clay mixtures with different pore fluids, Eng. Geol., 164, pp. 36-49, https://doi.org/10.1016/j.enggeo.2013.06.011.
[11] Cabalar, A.F., Mustafa, W.S. (2015). Fall cone tests on clay–sand mixtures, Eng. Geol., 192, pp.154-165, https://doi.org/10.1016/j.enggeo.2015.04.009.

[12] Elkady, T.Y., Shaker, A.A. and Dhowain, A.W., (2015). Shear strengths and volume changes of sand–attapulgite clay mixtures, Bull. Eng. Geol. Environ.74, pp. 595–609.
[13] Mun, W., Balci, M.C., Valente, F. and McCartney, JS. (2018). Shearing and compression behavior of compacted sand-clay mixtures. Proceeding of the 7th International Conference on Unsaturated Soils UNSAT 2018, Hong Kong university.
[14] Sun, D., Sun, W., Yan, W. and Li, J. (2010). Hydro-mechanical behaviours of highly compacted sand-bentonite mixture, J. Rock Mech. Geotech. Eng., 2(1), pp. 79–85. DOI:10.3724/SP.J.1235.2010.00079.
[15] Anuchit, U. (2014). Effect of suction on unconfined compressive strength of clayey soils with different sand contents, ARPN, J. Eng. Appl. Sc., 9(6), pp. 881-884. http://www.arpnjournals.com/jeas/volume_06_2014.htm.
[16] Khan, F. S., Azam, S., Raghunandan, M.E. and Clark, R. (2014). Compressive Strength of Compacted Clay-Sand Mixes, Adv. Mater. Sci. Eng., Volume 2014, Article ID 921815, 6 pages. DOI:10.1155/2014/921815.
[17] Serbah, B., Abou-Bekr, N., Bouchemella, S., Eid, J. and Taibi, S. (2018). Dredged sediments valorisation in CEBs: Suction and water content effect on their 1 mechanical properties, Constr. Build. Mater., 158, pp. 503–515. DOI:10.1016/j.conbuildmat.2017.10.043.
[18] Cabalar A.F., Khalaf, M.M. and Karabash, Z. (2018). Shear modulus of clay-sand mixtures using bender element test, Acta Geotech. Slov., (1), pp. 3-15. DOI:10.18690/actageotechslov.15.1.3-15.2018.
[19] Kenney, T.C., Van Veen, W.A., Swallow, M.A., and Sungaila, M.A. (1992). Hydraulic conductivity of compacted bentonite sand mixtures, Can. Geotech. J. 29(3), 364- 374. DOI:10.1139/t92-042.
[20] Howell, J.L., Shackeford, C.D., Amer, N.H. and Stern, R.T. (1997). Compaction of sand-10 processed clay soil mixtures, Geotech. Test. J., 20(4), pp. 443-458. DOI: 10.1520/GTJ10411J.
[21] Colmenares Montanes, J.E. (2002). suction and volume changes of compacted sand-bentonite mixtures, PH.D Thesis., university of London, U.K
[22] Cabalar, A.F., Mustafa, W.S. (2017). Behaviour of sand–clay mixtures for road pavement subgrade, Int. J. Pavement Eng., 18(8), 714-726. DOI: 10.1080/10298436.2015.1121782
[23] Sivapullaiah P., Sridharan, A. and Stalin, V.k. (2000). Hydraulic Conductivity of Bentonite Sand Mixtures, Can. Geotech. J., 37(2), pp. 406-413, DOI:10.1139/T99-120.
[24] Fuentes, W.M., Hurtado, C. and Lascarro, C. (2018). On the influence of the spatial distribution of fine content in the hydraulic conductivity of sand-clay mixtures, Earth Sci. Res. J., 22(4), pp. 239-249, DOI:10.15446/esrj.v22n4.69332.
[25] Taibi, S. (1994). Comportement mécanique et hydraulique des sols soumis à une pression interstitielle négative – Etude expérimentale et modélisation, Ph.D. Thesis, Ecole centrale, Paris, France.
[26] Fleureau, J.-M., Verbrugge, J.-C., Huergo, P.J, Correia, A.-G. and Kheirbek-Saoud, S. (2002). Aspects of the behaviour of compacted clayey soils on drying and wetting paths, Can. Geotech. J. 39(6), pp. 1341–1357. DOI:10.1139/t02-100.
[27] Hattab, M. and Fleureau, J.M. (2010). Experimental study of kaolin particle orientation mechanism, Géotechnique 60(5), pp. 323-331. DOI:10.1680/geot.2010.60.5.323.
[28] Wei X., Hattab M., Fleureau, J.M. and Ruilin, H. (2013). Micro–macro experimental study of two clayey materials on drying paths, Bull. Eng. Geol. Environ. 72(3–4), pp. 495–508. DOI:10.1007/s10064-013-0513-4.
[29] Ighil Ameur, L., Robin, R. and Hattab, M. (2016). Elastic properties in a clayey material under mechanical loading - an estimation through ultrasonic propagations, Eur. J. Environ. Civ. Eng., 20 (9), pp. 1127-1146. DOI:10.1080/19648189.2015.1090926.
[30] NF EN ISO 17892-4 (2018), Geotechnical investigation and testing - Laboratory testing of soil - Part 4: Determination of particle size distribution. French standard, AFNOR Editions. France.
[31] NF EN ISO 17892-12 (2018). Geotechnical investigation and testing - Laboratory testing of soil - Part 12: determination of liquid and plastic limits. French standard, AFNOR Editions. France.
[32] Tan, T.S., Goh, T.C., Karunaratne, G.P., Lee, S.L., (1994). Shear strength of very soft clay–sand mixtures. Geotech. Test. J., 17(1), pp.27–34.
[33] Kheirbek-Saoud, S. (1994). Comportement mécanique de la couche de fondation d'une voie ferrée. Ph.D. Thesis, Ecole centrale de Paris, Paris, France.
[34] NF P94-093 (2014). Soils: investigation and testing - Determination of the compaction reference values of a soil type - Standard proctor test - Modified Proctor test, French standard, AFNOR Editions. France.
[35] Azam, S. and Chowdhury, R. H. (2013). Swell-shrink-consolidation behaviour of compacted expansive clays, Int. J. Geot. Eng., 7(4), pp. 424–430.
[36] Marinho, F. A. M. and Oliveira, O. M. (2012). Unconfined shear strength of compacted unsaturated plastic soils, Proceedings of the Institution of Civil Engineers: Geot. Eng., 165(2), pp. 97–106.
[37] NF EN ISO 17892-7 (2018). Geotechnical investigation and testing - Laboratory testing of soil - Part 7: unconfined compression test, French standard, AFNOR Editions. France.
[38] NF EN ISO 17892-9 (2018). Geotechnical investigation and testing - Laboratory testing of soil - Part 9: consolidated triaxial compression tests on water saturated soils, French standard, AFNOR Editions. France.
[39] Taibi, S., Duperret, A. and Fleureau, J.-M. (2009). The effect of suction on the hydro mechanical behaviour of chalk rocks, Eng. Geol., 106, pp.40–50.
[40] Biarez, J., Fleureau, J.M., Zerhouni, M.I and Soepandji, B.S. (1988). Variations de volume des sols argileux lors de cycles de drainage-humidification. Revue Française de Géotechnique, 41, pp. 63-71.
[41] Fleureau, J.M., Kheirbek-Saoud, S., Soemitro, R. and Taibi, S. (1993). Behavior of clayey soil on drying-wetting paths. Can. Geotech. J., 3(2), 287 -296. https://doi.org/10.1139/t93-024.
[42] Zur, B. (1966). Osmotic control the matrix soil water potential, Soil Sci., pp. 394–398.
[43] Williams, J. and Shaykewich, C.F. (1969). An evaluation of polyethylene glycol (P.E.G.) 6000 and P.E.G. 20000 in the osmotic control of soil water matrix potential, Can. J. Soil Science, 102, pp. 394–398.
[44] Indarto (1991). Comportement mécanique et compactage des matériaux de barrages. Ph.D. Thesis, Ecole centrale de Paris, Paris, France.

[45] Delage, P. and Suraj, D. (1992). Suction controlled testing of non-saturated soils with osmotic consolidometer. 7th international conference expansive soils, Dallas, pp. 206–211.
[46] Delage, P., Howat, M.D. and Cui, Y.J. (1998). The relationship between suction and swelling properties in a heavily compacted unsaturated clay, Eng. Geol., 1(1), pp. 31-48. DOI: 10.1016/S0013-7952(97)00083-5
[47] Bouchemella, S. and Alimi-Ichola, I. (2016). Détermination de la variation spatio-temporelle de la teneur en eau lors d'une infiltration verticale en utilisant la méthode TDR, Annales du Bâtiment et des Travaux Publics. 68 (5-6). Numéro spécial : 34es Rencontres universitaires de Génie Civil, Liège, 24-27 mai 2016. ISBN 978-2-7472-2690-5 (ISSN 1270-9840).
[48] ASTM D5298-16 (2016). Standard Test Method for Measurement of Soil Potential (Suction) Using Filter Paper, ASTM International, West Conshohocken, PA., USA. DOI: 10.1520/D5298-16.
[49] Muhwezi, L. and Achanit, S. E. (2019). Effect of Sand on the Properties of Compressed Soil-Cement Stabilized Blocks. Colloid and Surface Science. 4(1), pp.1-6. DOI: 10.11648/j.css.20190401.11
[50] Mullins, C.E. and Panayiotopoulos, K.P. (1984). The strength of unsaturated mixtures of sand and kaolin and the concept of effective stress, J. Soil Sci., 35(3), pp. 459–468.